

Field-induced transverse spin ordering in FeBr₂

O. Petracic, Ch. Binek, and W. Kleemann

Laboratorium für Angewandte Physik, Gerhard-Mercator-Universität Duisburg, D-47048 Duisburg, Germany

U. Neuhausen and H. Lueken

Institut für Anorganische Chemie, Rheinisch-Westfälische Technische Hochschule, D-52074 Aachen, Germany

(Received 5 March 1998)

Weak first-order phase transitions from axial to oblique spin ordering in FeBr₂ are evidenced by superconducting quantum interference device magnetometry in axial fields $H_1(T)$ above the multicritical point, $H_m = 2.4$ MA/m, $T_m = 4.6$ K, and below the antiferro-to-paramagnetic phase line, $H_c(T)$, in agreement with recent specific-heat data [H. Aruga Katori, K. Katsumata, and M. Katori, Phys. Rev. B **54**, R9620 (1996)]. The ordering of the in-plane moments is probably due to nondiagonal coupling to the longitudinal ones, both of which increase discontinuously at $H_1(T)$ only under an additional symmetry-breaking transverse field. [S0163-1829(98)52118-2]

Antiferromagnetic (AF) materials with competing exchange interactions in addition to strong or intermediate uniaxial anisotropy have been of vivid interest for a long time.¹⁻³ Recently increased attention has been paid to the axial magnetic phase diagram of the layered insulating compound FeBr₂. Magnetometric investigations of de Azevedo *et al.*⁴ have shown that the well-known magnetic field-induced second-order phase line $H_c(T)$ between the Néel ($T_N = 14.1$ K, $H = 0$) and the multicritical point (MCP, $T_m = 4.6$ K, $H_m = 2.4$ MA/m),⁵ is preceded by large noncritical anomalies. As shown in Fig. 1 they peak on the anomaly line $H_-(T)$, which joins the critical one, $H_c(T)$, at the MCP (arrow). They are attributed to spin fluctuations on that sublattice, the magnetization of which is antiparallel to \mathbf{H} in the low-field limit. As pointed out by Selke and co-workers,⁶⁻⁸ the main reason for this peculiarity is the relatively weak, albeit dominating, intraplanar ferromagnetic interaction, J , in comparison with the AF interplanar exchange, J' . In addition the large number of nearest interplanar neighbor spins $z' = 20$, compared with the in-plane situation, $z = 6$, seems to be crucial for the unusual fluctuation peaks. They appear both in the magnetic susceptibility and in the magnetic specific heat within mean-field approximation^{6,7} and Monte Carlo simulations of Ising models with realistic interaction parameters.⁸ In the paramagnetic (PM) precursor region noncritical fluctuations are observed as well along the line $H_+(T)$ (Fig. 1) both in experiments^{4,9} and simulations.⁸

The magnetic specific heat recently has been measured by Aruga Katori *et al.*¹⁰ Surprisingly, sharp spikes were found at fields $H_1(T)$ slightly above the anomaly line $H_-(T)$ (Fig. 1). $H_1(T)$ is regarded as a new phase line extending between the MCP (now interpreted as a critical endpoint, CEP) and a bicritical endpoint (BCE, $T_{BCE} \approx 11$ K, $H_{BCE} \approx 1.1$ MA/m).¹¹ It seems to comply with calculations on a certain class of anisotropic Heisenberg antiferromagnets³ and to confirm recent quantum Monte Carlo calculations on a Hubbard model adapted to FeBr₂.^{12,13} Remarkably, however, neither magnetometric measurements in axial magnetic fields^{4,9} nor comprehensive calculations within various Ising-type approaches^{7,8} have ever shown phase transitionlike phenom-

ena in addition to the short-range order fluctuations reflected by the noncritical peaks at H_- and H_+ . By mutual exchange of samples between RIKEN^{10,11} and the University of Duisburg^{4,9} it has been ascertained that the different signatures of specific heat and susceptibility data are not due to different sample quality.

Previously the relevance of the transverse spin components has been inferred from Mössbauer spectroscopical data on FeBr₂ (Ref. 14) for fields ranging between H_- and H_c . Hence it appears tempting to assume a phase transition at H_1 involving merely the transverse spin components without affecting the longitudinal magnetization. In this case criticality of intraplanar spin-spin correlation functions is expected, which should contribute to the specific heat, C_m , as observed.¹⁰ This conjecture is readily verified by a relation-

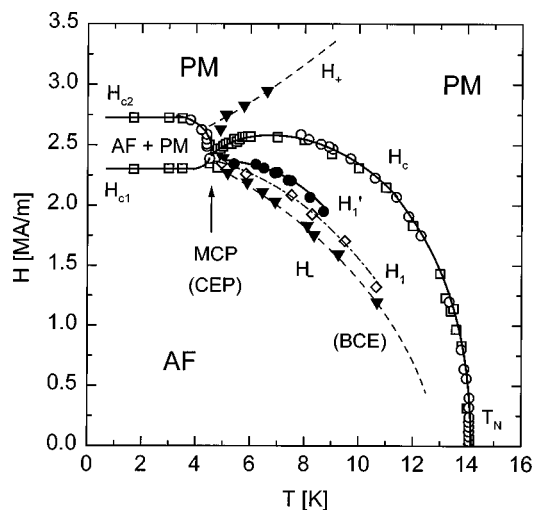


FIG. 1. H - T -phase diagram of FeBr₂ (Ref. 4), where H is the applied axial magnetic field. The phase lines H_c , H_{c1} , H_{c2} , H_- , and H_+ vs T refer to measurements of M vs H (open squares), M vs T (open circles), and χ'' vs T (solid triangles). H_1 and H'_1 vs T denote the positions of the spikes found by specific heat (open diamonds) (Ref. 10) and off-axis magnetization measurements (solid circles; see Fig. 3), respectively.

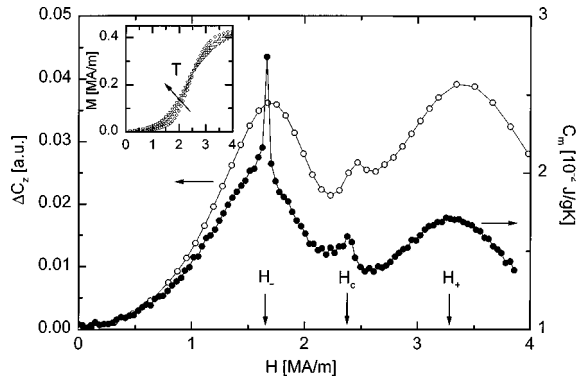


FIG. 2. Calculated curve (see text), $\Delta C_z(H)$, for $T=9.0$ K (open circles) and measured magnetic specific heat, $C_m(H)$, of FeBr_2 for $T=9.3$ K (Ref. 17) (solid circles). H_- , H_c , and H_+ are indicated by arrows. The inset shows $M_z(H)$ data measured at $T=8, 9$, and 10 K (arrow) and used for the calculations.

ship between the longitudinal magnetization, $M_z(H, T)$, and its contribution to C_m ,

$$\Delta C_z(H) = C_z(H, T) - C_z(H=0, T) = T \int_0^H \frac{\partial^2 M_z}{\partial T^2} dH', \quad (1)$$

which is based on Maxwell's relation $\partial M / \partial T = \partial S / \partial H$.^{15,16} In Fig. 2 we show the specific heat as calculated via Eq. (1) from M_z data measured in the vicinity of $T=9$ K (see inset) in comparison with experimental data of the specific heat, $C_m(H)$, obtained by caloric measurements at $T=9.3$ K.¹⁷ Both curves agree in showing broad noncritical peaks at H_- and H_+ , and the critical peak at H_c (1.7, 3.4, and 2.4 MA/m, respectively), slight differences being due to the slightly different temperatures involved. However, the sharp spike appearing at $H_1=1.7$ MA/m in C_m is definitely missing in ΔC_z . Within errors this transitionlike phenomenon seems to originate in transverse magnetic ordering processes, which are virtually not contributing to the axial magnetization component.

In order to detect the conjectured transverse spin ordering, we have measured the magnetization in both the longitudinal and the transverse directions under the control of an intraplanar field component, H_{pl} , in addition to a sufficiently large axial field component, $H_- < H_{ax} < H_c$. In fact, under these circumstances discontinuities of both components of $\mathbf{M}(T)$ are encountered. They clearly hint at ordering of the transverse spin components. Figure 3 shows the temperature dependences of the magnetization components parallel and perpendicular with respect to the external field, $M_{\parallel}(T)$ and $M_{\perp}(T)$, respectively. They are obtained with a superconducting quantum interference device (SQUID) allowing one to detect longitudinal and transverse magnetic moments (Quantum Design, MPMS-5S) on an as-cleft single crystal platelet of FeBr_2 (size $5 \times 2 \times 0.4$ mm³). It is inclined with its crystallographic c axis (perpendicular to the large face) under an angle $\theta=(33 \pm 2)^\circ$ with respect to the applied longitudinal field, \mathbf{H} , choosing $H=2.63, 2.71$, and 2.79 MA/m with axial and planar components, $H_{ax}=H \cos \theta=2.20, 2.27$, and 2.34 MA/m and $H_{pl}=H \sin \theta=1.43, 1.48$, and 1.52 MA/m (Fig. 3, sketch).

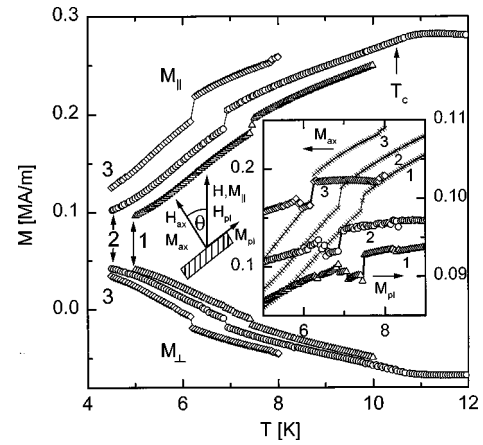


FIG. 3. M_{\parallel} and M_{\perp} vs T measured in fields $H=2.63$ (1), 2.71 (2), and 2.79 MA/m (3) on a sample of FeBr_2 inclined by $\theta=33^\circ$. The orientations of field and magnetization components are denoted in a sketch. The inset shows M_{ax} (crosses) and M_{pl} (open symbols; jumps marked by vertical lines) vs T as calculated from M_{\parallel} and M_{\perp} .

As expected, M_{\parallel} is positive at all T and reaches maximum slope at $T_c(H)$, e.g., at $T_c(H_{ax}=2.27 \text{ MA/m})=10.8$ K (arrow). On the other hand, M_{\perp} changes its sign as T increases. This is due to the superposition of a positive planar (M_{pl}) and a negative axial component (M_{ax}) of the magnetization (Fig. 3, sketch). Whereas M_{pl} is virtually constant ($\chi_{\perp} \approx \text{constant}$), $|M_{ax}|$ increases with increasing T in parallel with $M_{\parallel}(T)$. Surprisingly, both magnetization components clearly show weak abrupt jumps, positive for M_{\parallel} and negative for M_{\perp} , at distinct temperatures, $T_1=7.4, 6.9$, and 6.2 K, respectively. When calculating the magnetization components referring to the sample coordinates, however, both $M_{ax}=M_{\parallel} \cos \theta - M_{\perp} \sin \theta$ and $M_{pl}=M_{\parallel} \sin \theta + M_{\perp} \cos \theta$ are found to increase discontinuously at $T_1(H_{ax})$ (Fig. 3, inset). The excessive noise preceding the very small jumps of M_{pl} is due to systematic errors encountered in very small SQUID signals, $M_{\perp} \approx 0$.

Let us first remark that the jump heights of both M components are (within errors) proportional to one another and that they decrease with decreasing field. Within experimental accuracy they seem to disappear at $T_1(H_{ax}=1.95 \text{ MA/m})=8.7$ K. A plot of T_1 vs H_{ax} as a line $H'_1(T)$ in Fig. 1 turns out to nearly coincide with the phase line $H_1(T)$.¹⁰ It remains to be shown by higher resolution magnetometry that $H'_1(T)$ eventually extends up to $T_{BCE} \approx 11$ K as in the caloric measurements.¹⁰ Second, it seems obvious that only the axial field component is decisive for the occurrence of the phase transition at $H_1(T)$. Figure 4 shows two curves dM_{\parallel}/dT vs T obtained with the same axial field, $H_{ax}=2.16$ MA/m, but under different tilting angles, $\theta=0^\circ$ and 30° . Both curves nearly coincide thus showing, in fact, that only the axial field component, $H_{ax}=H \cos \theta$, is responsible for the overall signature of dM_{\parallel}/dT . This concerns, in particular, the position of T_c (arrow), which is invariant under angular tilting provided that $H_{ax}=H \cos \theta$ remains constant. In addition, also the amplitude of the derivative of the axial magnetization, dM_{ax}/dT , seems to remain constant for constant H_{ax} . This is obvious from Fig. 4, where the 30° curve has been divided by $\cos(30^\circ)$. Only the projection $(dM_{ax}/dT) \cos \theta$ contrib-

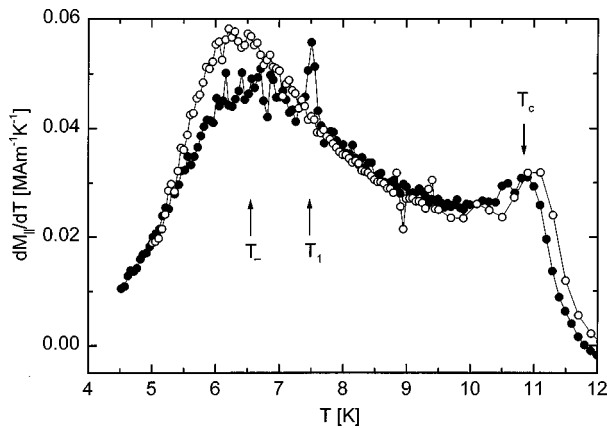


FIG. 4. $dM_{||}/dT$ vs T measured in the same axial field $H_{ax} = 2.16$ MA/m with tilting angles $\theta = 0^\circ$ (open symbols) and 30° (solid symbols). The 30° data are divided by $\cos(30^\circ)$. Peaks at T_- , T_1 , and T_c are indicated by arrows.

utes to $dM_{||}/dT$, whereas the contribution of the planar moment, $(dM_{pl}/dT)\sin\theta$, virtually vanishes (see Fig. 3, inset).

At a closer look, however, both curves in Fig. 4 reveal two important differences. On the one hand, a sharp spike is observed at $T_1 = 7.0$ K in the tilted configuration. On the other hand, the noncritical anomaly at $T_- = 6.5$ K shrinks significantly in this geometry. These observations clearly evidence that the axial spin components are responsible for the noncritical fluctuations in accordance with all Ising model calculations hitherto available,^{6–8,10} whereas the weak first-order anomaly is exclusively affected by the transverse spin components. Thus an ordinary spin-flop transition at $H_1(T)$ as predicted by conventional anisotropic Heisenberg models^{3,8} seems to be ruled out. It would primarily involve a jump of the longitudinal magnetization accompanied by the appearance of transverse moments.

Our observations are more favorable towards a disorder-order transition of the $m_s = 0$ spin components when crossing the $H_1(T)$ phase line. The planar spin ordering probably originates from the off-diagonal exchange between axial and

planar spin components, S_{ax} and S_{pl} , respectively, which is allowed by symmetry.¹⁸ By virtue of ferromagnetic $S_{ax}S_{pl}$ coupling the secondary order parameter, $\langle S_{pl} \rangle$, appears discontinuously at the critical field $H_1(T)$, where the field-induced ferromagnetic order parameter, $\langle S_{ax} \rangle$, attains sufficiently large values. The expected¹⁹ rotational XY symmetry of $\langle S_{pl} \rangle$ is probably broken by magnetocrystalline anisotropy and magnetoelastic coupling.²⁰ In order to observe $\langle S_{pl} \rangle \neq 0$, however, a uniaxial in-plane field is required, which lifts the remaining degeneracy. In this case the discontinuity of $\langle S_{pl} \rangle$ causes a corresponding one of $\langle S_{ax} \rangle$. Hints at in-plane anisotropy are already obvious from our present data. The discontinuities, $\delta M_{||}$, shown in Figs. 3 and 4 for different samples with similar dimensions under the same conditions ($H_{ax} \approx 2.2$ MA/m, $\theta \approx 30^\circ$) differ by nearly one order of magnitude. Presumably easy and hard intraplanar axes, respectively, were hit fortuitously in these experiments. It will be interesting to study these and other details of the transverse spin ordering, e.g., by neutron scattering and by transverse susceptibility measurements both with and without an orientating planar field.

To summarize, by measuring the transverse components of the magnetic moment in a preponderantly axial magnetic field the puzzling discrepancy between longitudinal magnetization and magnetic specific heat of FeBr₂ has been clarified. Transverse spin ordering takes place along a first-order phase line $H_1(T)$ in the range $4.6 \text{ K} \leq T < 11 \text{ K}$, whereas the longitudinal magnetization varies continuously at $H_1(T)$. Probably the transverse transition involves nondiagonal exchange between the orthogonal spin components. They order mutually when applying an additional orientating transverse field.

Thanks are due to H. Aruga Katori, RIKEN, Wako, for allowing us to present her specific heat data prior to publication, to H. Junge for crystal growth of FeBr₂, and to the Deutsche Forschungsgemeinschaft (Graduiertenkolleg ‘‘Struktur und Dynamik heterogener Systeme’’ at Duisburg and SQUID magnetometer at Aachen) for financial support.

- ¹J. M. Kincaid and E. G. D. Cohen, Phys. Rep., Phys. Lett. **22C**, 57 (1975).
- ²E. Strykowski and N. Giordano, Adv. Phys. **26**, 487 (1997).
- ³I. Vilfan and S. Galam, Phys. Rev. B **34**, 6428 (1986).
- ⁴M. M. P. de Azevedo, Ch. Binek, J. Kushauer, W. Kleemann, and D. Bertrand, J. Magn. Magn. Mater. **140-144**, 1557 (1995).
- ⁵A. R. Fert, P. Carrara, M. C. Lanusse, G. Mischler, and J. P. Redoulès, J. Phys. Chem. Solids **34**, 223 (1973).
- ⁶W. Selke and S. Dasgupta, J. Magn. Magn. Mater. **147**, L245 (1995).
- ⁷W. Selke, Z. Phys. B **101**, 145 (1996).
- ⁸M. Pleimling and W. Selke, Phys. Rev. B **56**, 8855 (1997).
- ⁹O. Petracic, Ch. Binek, and W. Kleemann, J. Appl. Phys. **81**, 4145 (1997).
- ¹⁰H. Aruga Katori, K. Katsumata, and M. Katori, Phys. Rev. B **54**, R9620 (1996).
- ¹¹K. Katsumata, H. Aruga Katori, S. M. Shapiro, and G. Shirane, Phys. Rev. B **55**, 11 466 (1997).
- ¹²K. Held, M. Ulmke, and D. Vollhardt, Mod. Phys. Lett. B **10**, 203 (1996).
- ¹³K. Held, M. Ulmke, N. Blümer, and D. Vollhardt, Phys. Rev. B **56**, 14 469 (1997).
- ¹⁴J. Pelloth, R. A. Brand, S. Takele, M. M. P. de Azevedo, W. Kleemann, Ch. Binek, J. Kushauer, and D. Bertrand, Phys. Rev. B **52**, 15 372 (1995).
- ¹⁵H. Mitamura, T. Sakakibara, G. Kido, and T. Goto, J. Phys. Soc. Jpn. **64**, 3459 (1995).
- ¹⁶Ch. Binek (unpublished).
- ¹⁷H. Aruga Katori and K. Katsumata (unpublished).
- ¹⁸D. Mukamel, Phys. Rev. Lett. **46**, 845 (1981).
- ¹⁹M. E. Lines, Phys. Rev. **131**, 540 (1963).
- ²⁰W. Nitsche and W. Kleemann, Phys. Rev. B **36**, 8587 (1987).